bioRxiv preprint doi: https://doi.org/10.1101/2023.10.19.563168; this version posted February 17, 2024. The copyright holder for this preprint (which was not certified by peer review) is the author/funder, who has granted bioRxiv a license to display the preprint in perpetuity. It is made available under aCC-BY-NC-ND 4.0 International license.

Supplementary Methods and Results

RNA-sequencing analysis of isolated dorsal striatal microglia.

Biological replicates determined to be outliers were removed for differential gene expression analysis (**Supplementary Fig. 3A**). Principal component analysis (PCA) (**Supplementary Fig. 3B**) and heatmap of hierarchical clustering of conditions based on gene expression (**Supplementary Fig. 3C**) shows high similarity of samples within condition, and that animals exposed to methamphetamine (Maintenance and Abstinence) cluster more closely than to Saline.

Microglia are not required for natural food reinforcement.

To test if microglia are necessary for learned operant behavior, we food-trained mice up to FR5 for 8 consecutive days (**Supplementary Fig. 5**). Mice were treated with PLX5622 (1200 ppm in AIN-76A chow) for the duration of the experiment. Microglial ablation does not affect natural food reinforcement in number of rewards earned (**Supplementary Fig. 5A**) (Two-way RM ANOVA; AIN-76A vs PLX5622, $F(1, 13) = .073$, $p = .791$) or lever discrimination (**Supplementary Fig. 5B**) (Two-way RM ANOVA; Active vs Inactive Lever, $F(3, 26) = 24.38$, $p < .0001$) and time to acquire operant lever pressing behavior (**Supplementary Fig. 5B**) (Two-way RM ANOVA; AIN-76A vs PLX5622, $F(1, 13) = .385$, $p = .545$).

bioRxiv preprint doi: https://doi.org/10.1101/2023.10.19.563168; this version posted February 17, 2024. The copyright holder for this preprint (which was not certified by peer review) is the author/funder, who has granted bioRxiv a license to display the preprint in perpetuity. It is made available under aCC-BY-NC-ND 4.0 International license.

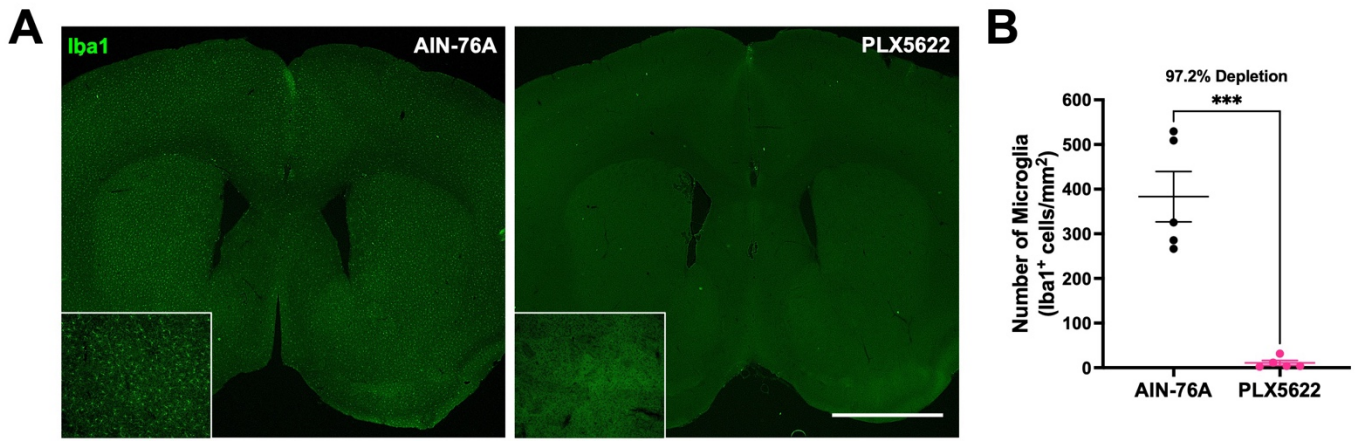

Supplementary Figure 1. Treatment with CSF1R inhibitor PLX5622 results in near complete depletion of microglia. A) Representative fluorescent images of Iba1$^+$ microglia (green) in the dorsal striatum from AIN-76A and PLX5622-treated mice. **B)** Quantification of microglial density. Unpaired t-test (AIN-76A vs PLX5622, ***$p < .001$). n = 5 per group. Data are represented as mean ± SEM. Scale bar = 1360 µm.

bioRxiv preprint doi: https://doi.org/10.1101/2023.10.19.563168; this version posted February 17, 2024. The copyright holder for this preprint (which was not certified by peer review) is the author/funder, who has granted bioRxiv a license to display the preprint in perpetuity. It is made available under aCC-BY-NC-ND 4.0 International license.

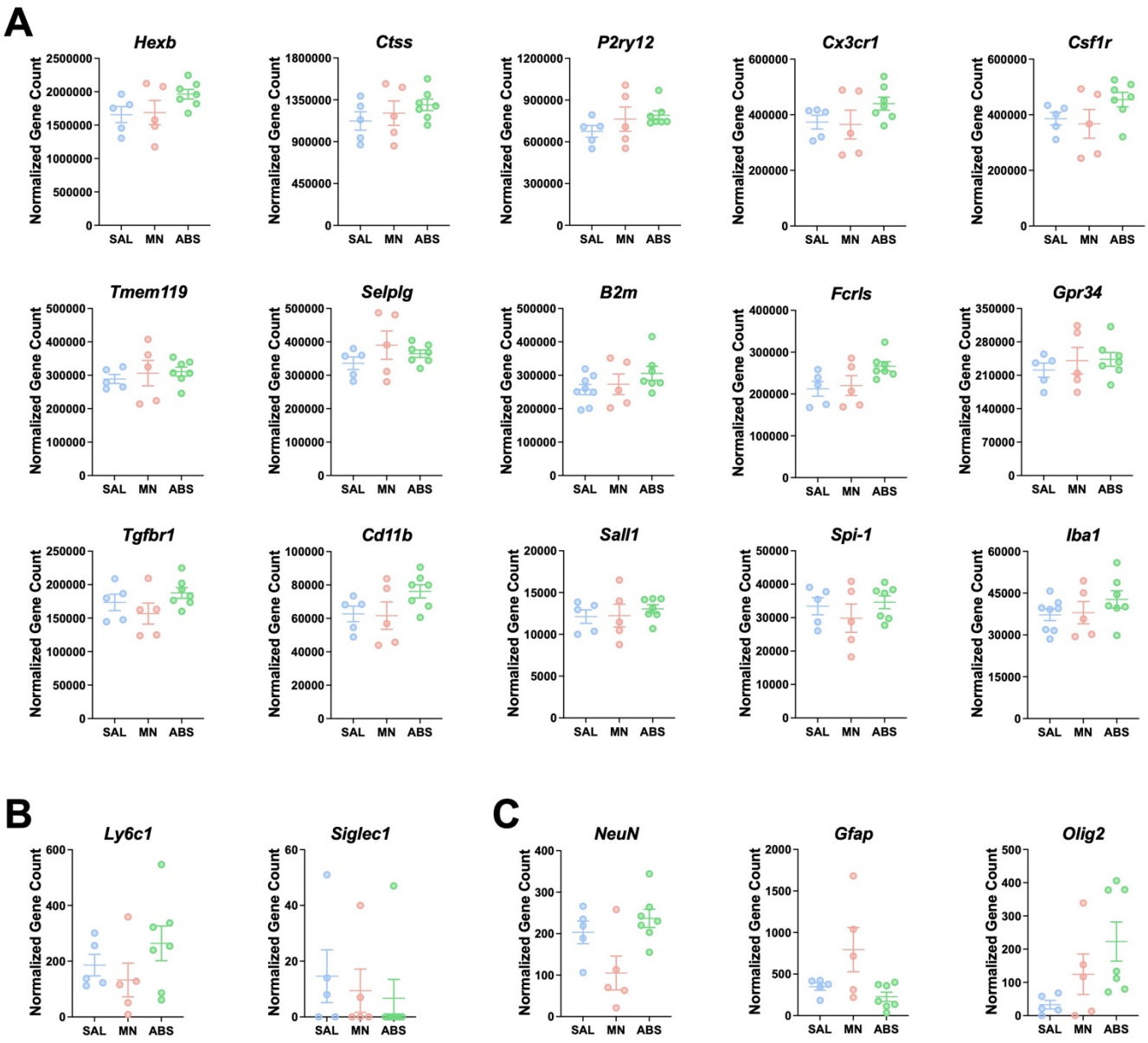

Supplementary Figure 2. Purity of isolated dorsal striatal microglia. A) Normalized counts of microglia-specific genes. **B)** Normalized counts of macrophage-specific genes. **C)** Normalized counts of other neural cell types-specific genes: neurons (*NeuN*), astrocytes (*Gfap*), oligodendrocytes (*Olig2*).

bioRxiv preprint doi: https://doi.org/10.1101/2023.10.19.563168; this version posted February 17, 2024. The copyright holder for this preprint (which was not certified by peer review) is the author/funder, who has granted bioRxiv a license to display the preprint in perpetuity. It is made available under aCC-BY-NC-ND 4.0 International license.

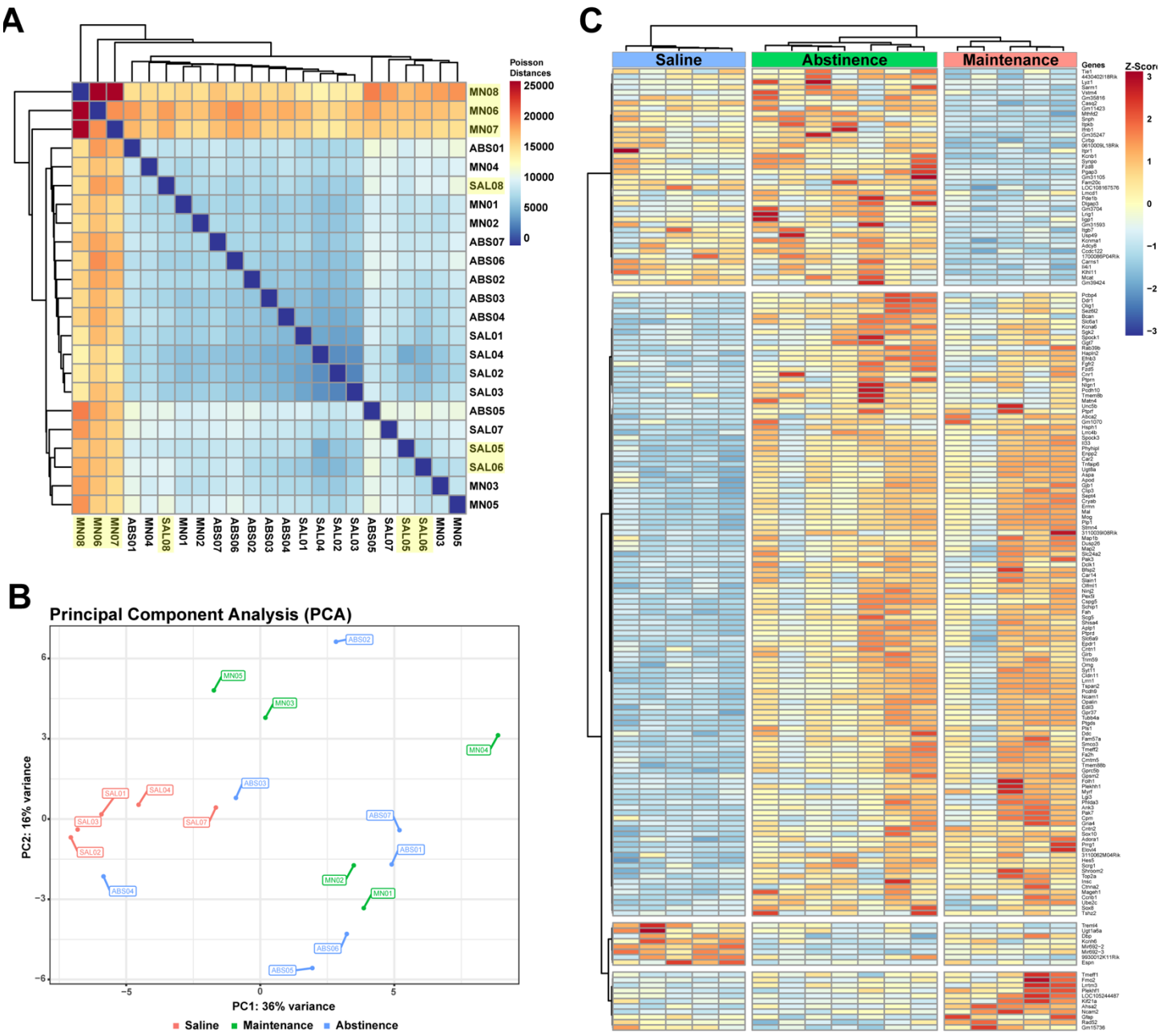

Supplementary Figure 3. RNA-sequencing of isolated dorsal striatal microglia from METH IVSA. A) Hierarchical clustering heatmap of expression profiles for samples (n = 23) based on Poisson distance. Highlighted samples were determined to be outliers and were removed from analyses. **B)** PCA plot for samples (n = 17) following removal of outliers. **C)** Heatmap showing unsupervised clustering of samples based on gene expression.

bioRxiv preprint doi: https://doi.org/10.1101/2023.10.19.563168; this version posted February 17, 2024. The copyright holder for this preprint (which was not certified by peer review) is the author/funder, who has granted bioRxiv a license to display the preprint in perpetuity. It is made available under aCC-BY-NC-ND 4.0 International license.

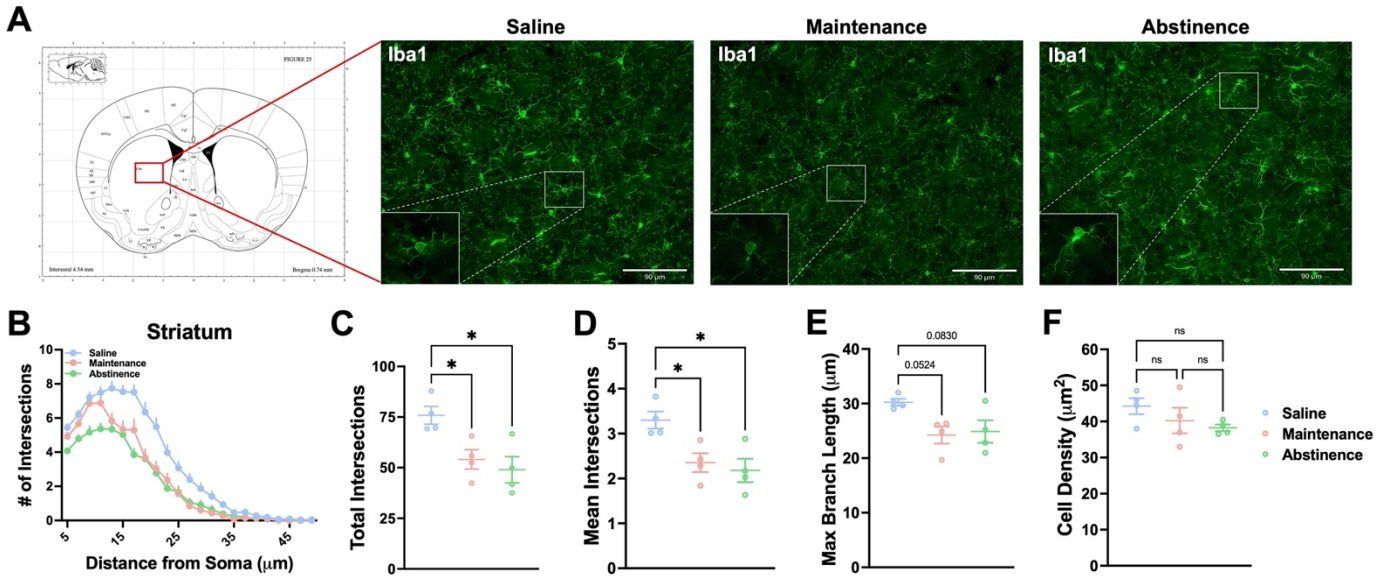

Supplementary Figure 4. Dorsal striatal microglia show persistent altered morphology due to METH administration. A) Representative fluorescent images (Bregma 0.74 mm, Paxinos and Franklin's the Mouse Brain in Stereotaxic Coordinates) of microglia ($Iba1^+$ cells) in the striatum. **B)** Sholl analysis plot of microglia. **C-F)** Mice that self-administered METH (Maintenance), as well as METH-abstinent mice (Abstinence), display less ramifications and branching complexity and shorter processes than Saline-taking mice (Saline), with no significant change in density. One-way ANOVA with Tukey post-hoc test (between conditions, $*p < .05$). n = 4 animals for all conditions. Data are represented as mean ± SEM. Scale bar = 90 μm.

bioRxiv preprint doi: https://doi.org/10.1101/2023.10.19.563168; this version posted February 17, 2024. The copyright holder for this preprint (which was not certified by peer review) is the author/funder, who has granted bioRxiv a license to display the preprint in perpetuity. It is made available under aCC-BY-NC-ND 4.0 International license.

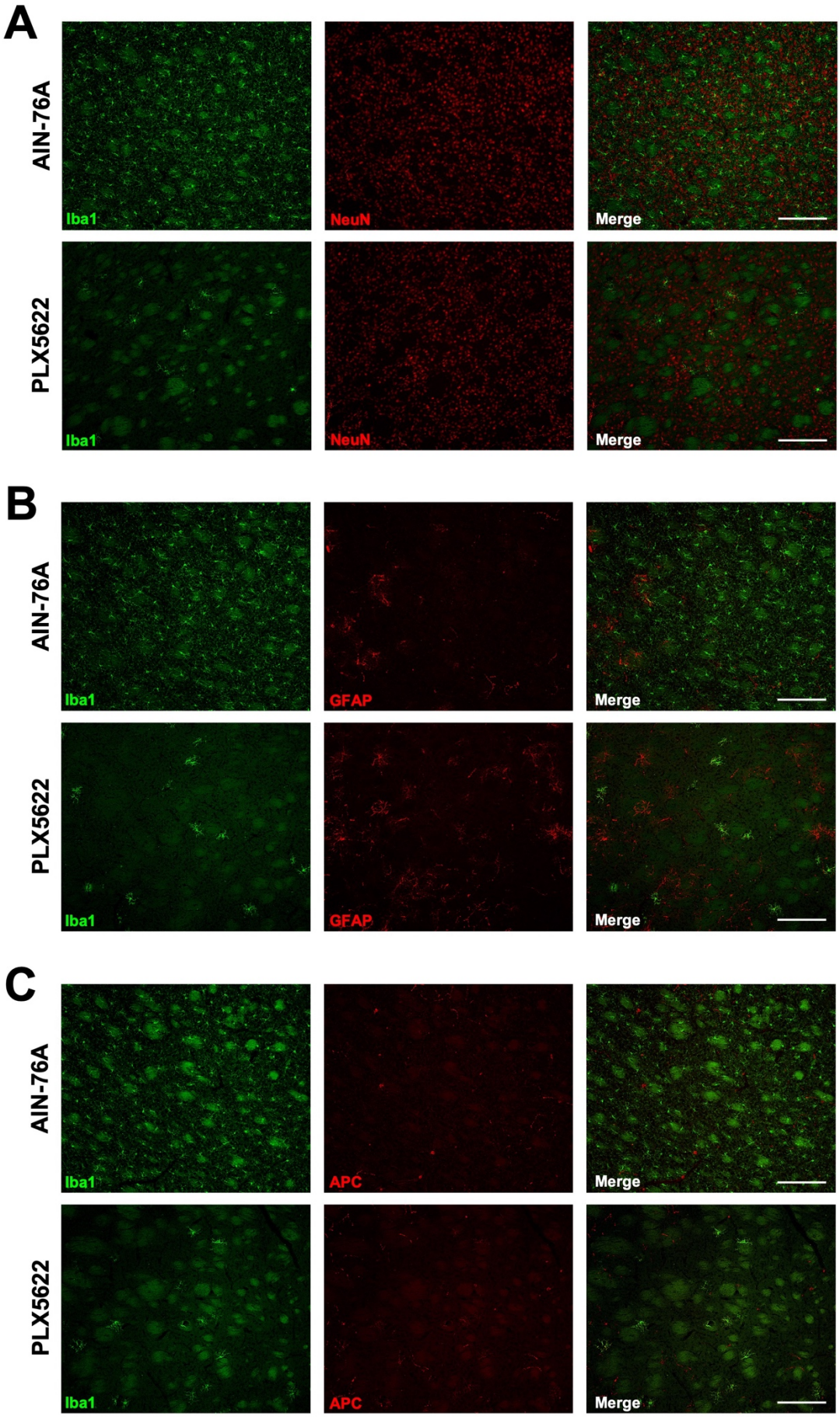

bioRxiv preprint doi: https://doi.org/10.1101/2023.10.19.563168; this version posted February 17, 2024. The copyright holder for this preprint (which was not certified by peer review) is the author/funder, who has granted bioRxiv a license to display the preprint in perpetuity. It is made available under aCC-BY-NC-ND 4.0 International license.

Supplementary Figure 5. PLX5622 treatment does not affect general morphology of neural cells in the dorsal striatum. A) Representative 10X images of microglia ($Iba1^+$, green) and neurons ($NeuN^+$, red). **B)** Representative 10x images of microglia ($Iba1^+$, green) and astrocytes ($GFAP^+$, red). **C)** Representative 10X images of microglia ($Iba1^+$, green) and oligodendrocytes (APC^+, red). Scale bar = 170 μm.

bioRxiv preprint doi: https://doi.org/10.1101/2023.10.19.563168; this version posted February 17, 2024. The copyright holder for this preprint (which was not certified by peer review) is the author/funder, who has granted bioRxiv a license to display the preprint in perpetuity. It is made available under aCC-BY-NC-ND 4.0 International license.

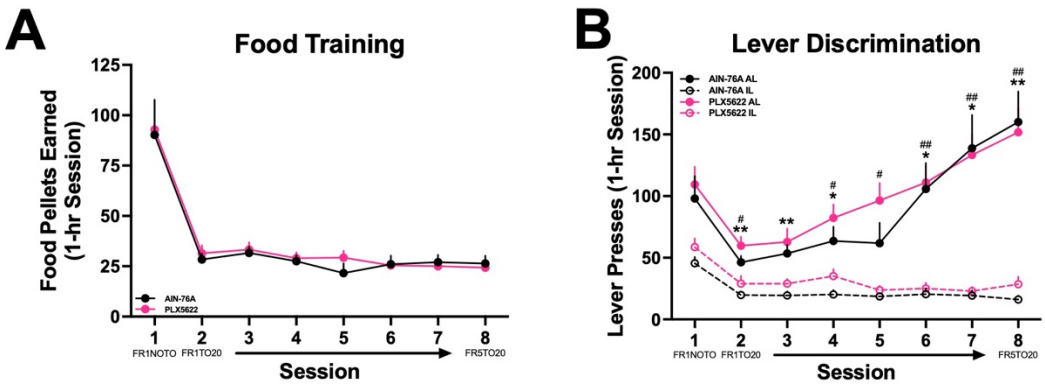

Supplementary Figure 6. Pharmacological ablation of microglia does not affect operant responding. **A)** Number of food rewards earned during 8 daily 1-hr sessions. **(B)** Active vs inactive lever presses during 8 daily 1-hr sessions (Two-way RM ANOVA with Bonferroni post-hoc test; AIN-76A Active vs Inactive Lever, *$p < .05$, **$p < .01$; PLX5622 Active vs Inactive Lever, $^{\#}p < .05$, $^{\#\#}p < .01$). AIN-76A (n = 8), PLX5622 (n = 7). Data are represented as mean ± SEM.

bioRxiv preprint doi: https://doi.org/10.1101/2023.10.19.563168; this version posted February 17, 2024. The copyright holder for this preprint (which was not certified by peer review) is the author/funder, who has granted bioRxiv a license to display the preprint in perpetuity. It is made available under aCC-BY-NC-ND 4.0 International license.

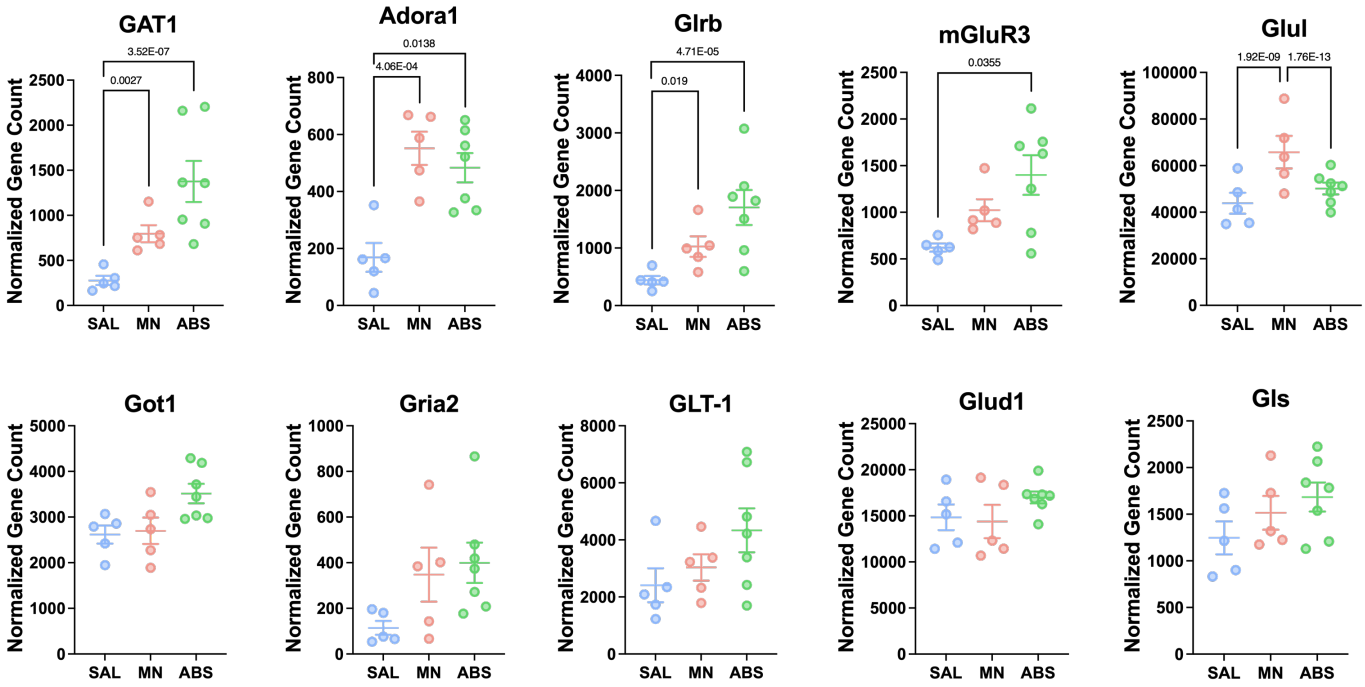

Supplementary Figure 7. GABA, glutamate, and adenosine signaling-related genes. Normalized counts of DE genes related to GABA, glutamate, and adenosine signaling with adjusted *p-value* for each comparison. Significance shown reflects pairwise comparison results from DESeq2.

bioRxiv preprint doi: https://doi.org/10.1101/2023.10.19.563168; this version posted February 17, 2024. The copyright holder for this preprint (which was not certified by peer review) is the author/funder, who has granted bioRxiv a license to display the preprint in perpetuity. It is made available under aCC-BY-NC-ND 4.0 International license.

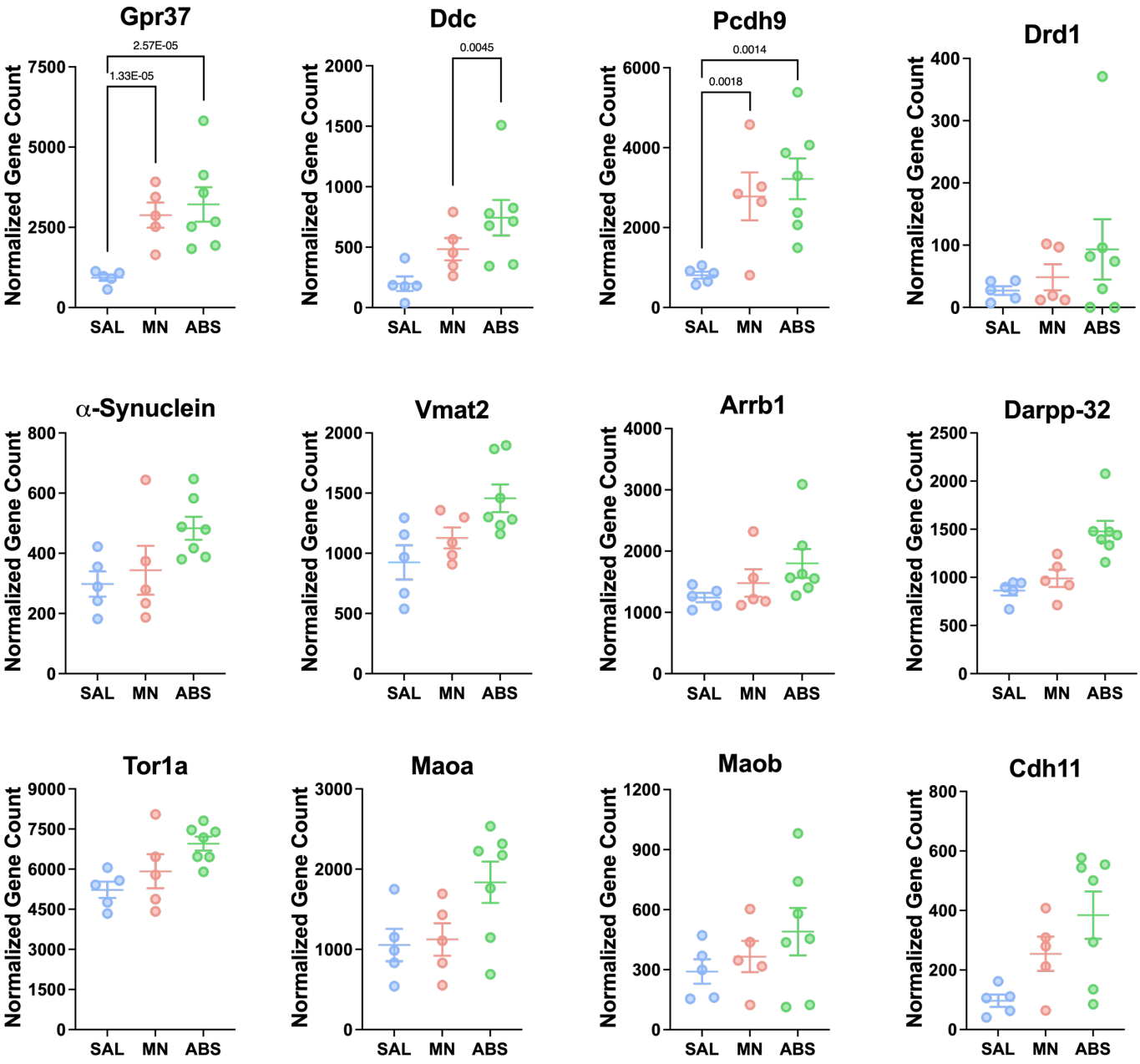

912

913 **Supplementary Figure 8. Dopamine signaling-related genes.** Normalized counts of DE genes with
914 adjusted *p-value* for each comparison. Significance shown reflects pairwise comparison results from
915 DESeq2.

916

bioRxiv preprint doi: https://doi.org/10.1101/2023.10.19.563168; this version posted February 17, 2024. The copyright holder for this preprint (which was not certified by peer review) is the author/funder, who has granted bioRxiv a license to display the preprint in perpetuity. It is made available under aCC-BY-NC-ND 4.0 International license.

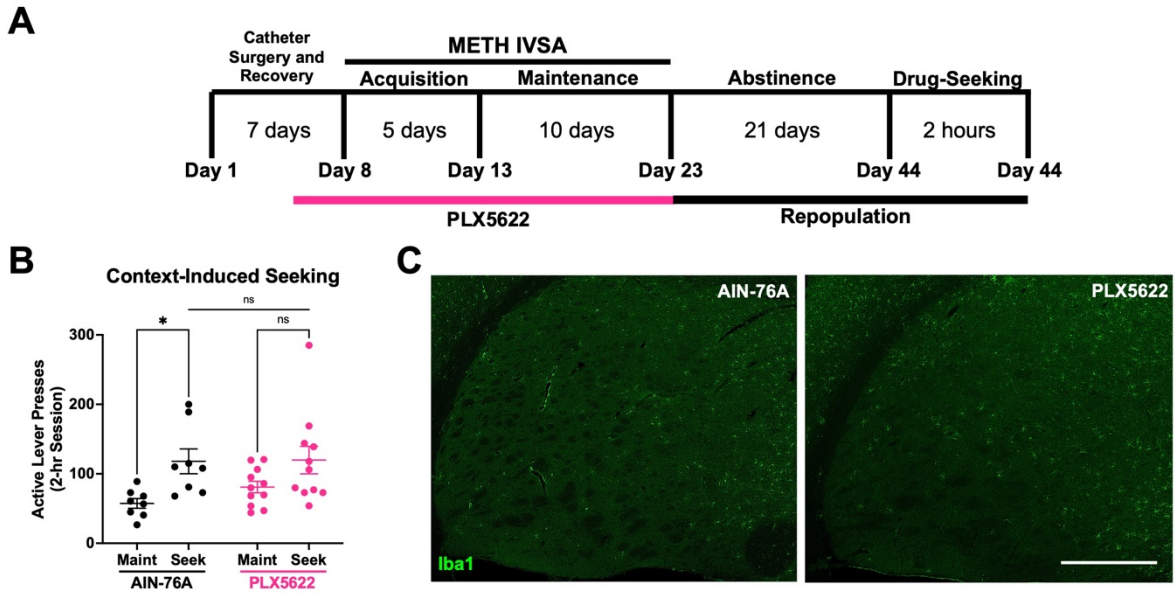

Supplementary Figure 9. Repopulation of microglia prevents context-induced drug-seeking. Mice were treated with PLX5622 for the duration of METH IVSA before being returned to control chow (AIN-76A) for the duration of abstinence. **A)** Experimental timeline. **B)** Active lever presses for Maintenance (**Maint**: average final 3 days) and Drug-Seeking (**Seek**) of AIN-76A and PLX5622. Two-way RM ANOVA with Bonferroni post-hoc test (AIN-76A Maint vs Seek, * $p < .05$; PLX5622 Maint vs Seek, $p = .144$; AIN-76A vs PLX5622 Seek, $p = .392$). **C)** Representative fluorescent images of Iba1$^+$ microglia (green) in the dorsal striatum from AIN-76A and PLX5622 treated mice. AIN-76A (n = 8), PLX5622 (n = 11). Data are represented as mean ± SEM. Scale bar = 470 μm.